Available online at www.sciencedirect.com
ScienceDirect
Solar Energy 81 (2007) 1340–1350
SOLAR ENERGY
www.elsevier.com/locate/solener

# A review on roughness geometry used in solar air heaters

Varun [a], R.P. Saini [b], S.K. Singal [b,*]

[a] Department of Mechanical Engineering, Moradabad Institute of Technology, Ram Ganga Vihar, Moradabad 244001, India
[b] Alternate Hydro Energy Centre, Indian Institute of Technology, Roorkee 247667, India

Received 16 June 2006; received in revised form 29 January 2007; accepted 31 January 2007
Available online 28 February 2007

Communicated by: Associate Editor Brian Norton

**Abstract**

The use of an artificial roughness on a surface is an effective technique to enhance the rate of heat transfer to fluid flow in the duct of a solar air heater. Number of geometries of roughness elements has been investigated on the heat transfer and friction characteristics of solar air heater ducts. In this paper an attempt has been made to review on element geometries used as artificial roughness in solar air heaters in order to improve the heat transfer capability of solar air heater ducts. The correlations developed for heat transfer and friction factor in roughened ducts of solar air heaters by various investigators have been reviewed and presented.


*Keywords:* Solar air heater; Artificial roughness; Effective efficiency; Heat transfer; Friction factor

## 1. Introduction

Energy in various forms has played an increasingly important role in world wide economic progress and industrialization. In view of the world's depleting fossil fuel reserves, which provide the major source of energy, the development of non-conventional renewable energy sources has received an impetus. Sunlight available freely as a direct and perennial source of energy provides a non-polluting reservoir of fuel. The simplest and the most efficient way to utilize solar energy is to convert it into thermal energy for heating applications by using solar collectors. Solar air heaters, because of their inherent simplicity are cheap and most widely used collection devices. The main applications of solar air heaters are space heating; seasoning of timber, curing of industrial products, and these can also be effectively used for curing/drying of concrete/clay building components. The solar air heater occupies an important place among solar heating system because of minimal use of materials and cost.

The thermal efficiency of solar air heaters in comparison of solar water heaters has been found to be generally poor because of their inherently low heat transfer capability between the absorber plate and air flowing in the duct. In order to make the solar air heaters economically viable, their thermal efficiency needs to be improved by enhancing the heat transfer coefficient. There are two basic methods for improving the heat transfer coefficient between the absorber plate and air. The first method involves increasing the area of heat transfer by using corrugated surfaces or extended surfaces called fins without affecting the convective heat transfer coefficient. The second method involves increasing the convective heat transfer by creating turbulence at the heat-transferring surface. This can be achieved by providing artificial roughness on the underside of absorber plate. Many investigators have attempted to design a roughness element, which can enhance convective heat transfer with minimum increase in friction losses.

* Corresponding author. Fax: +91 1332 273517.
*E-mail address:* sunilfah@iitr.ernet.in (S.K. Singal).

0038-092X/$ - see front matter © 2007 Elsevier Ltd. All rights reserved.
doi:10.1016/j.solener.2007.01.017

**Nomenclature**

| | | | |
|---|---|---|---|
| $D$ | equivalent diameter of the air passage (m) | $R$ | roughness function |
| $e$ | height of roughness element (m) | $Re$ | Reynolds number |
| $e^+$ | roughness Reynolds number | $S$ | length of main segment line of discrete rib element (m) (Fig. 6) |
| $e/D$ | relative roughness height | $s$ | shortway of mesh (m) (Fig. 5) |
| $f_r$ | friction factor of roughened duct | $s/e$ | relative shortway length of mesh |
| $f_s$ | friction factor of smooth duct | $\bar{S}t$ | average Stanton number |
| $G$ | momentum heat transfer function | $St_r$ | Stanton number of roughened duct |
| $H$ | height of duct (m) | $St_s$ | Stanton number of smooth duct |
| $l$ | longway of mesh (m) (Fig. 5) | $V$ | velocity of air in the duct (m/s) |
| $l/e$ | relative longway length of mesh | $W$ | width of duct (m) |
| $Nu_r$ | Nusselt number of roughened duct | | |
| $Nu_s$ | Nusselt number of smooth duct | | |
| $Pr$ | Prandtl number | *Greek symbols* | |
| $p$ | roughness pitch (m) (Figs. 1 and 2) | $\alpha$ | angle of attack of flow (°) (Fig. 4) |
| $p/e$ | relative roughness pitch | $\phi$ | wedge angle (°) (Figs. 8 and 9) |

## 2. Concept of artificial roughness

In order to attain higher heat transfer coefficient, it is desirable that the flow at the heat-transferring surface is made turbulent. However, energy for creating such turbulence has to come from the fan or blower and the excessive power required making the air flow through the duct. It is therefore desirable that the turbulence must be created only in the region very close to the heat transferring surface, i.e., in the laminar sub layer only where the heat exchange takes place and the flow should not be unduly disturbed so as to avoid excessive friction losses. This can be done by keeping the height of the roughness element small in comparison with the duct dimension. Although there are several parameters that characterize the arrangement and shape of the roughness, the roughness element height ($e$) and pitch ($p$) are the most important parameters. These parameters are usually specified in terms of dimensionless parameters, namely, relative roughness height ($e/D$) and the relative roughness pitch ($p/e$). The roughness elements can be two-dimensional ribs or three-dimensional discrete elements, transverse or angled ribs or V-shaped continuous or broken ribs. Although square ribs are the most commonly used geometry but chamfered, circular, semi-circular and grooved sections have been investigated in order to get most beneficial arrangement from thermohydraulic consideration.

### 2.1. Fluid flow and heat transfer characteristics of roughened surface

In view of the complex nature of the flow comprising separated turbulent flows produced by certain special orientations of the ribbed artificial roughness, it is difficult to develop analytical flow models. Early studies beginning with that of Nikuradse (1950) attempted to develop velocity and temperature distribution for roughened surfaces.

(i) For smooth surface

$$u^+ = y^+ \text{ for laminar sublayer}, \quad y^+ \leqslant 5 \tag{1}$$

$$u^+ = 5\ln y^+ + 3.5 \text{ for buffer layer}, \quad 5 \leqslant y^+ \leqslant 30 \tag{2}$$

$$u^+ = 2.5\ln y^+ + 5.5 \text{ for turbulent layer}, \quad y^+ > 30 \tag{3}$$

(ii) For roughened surface

A detailed study of the data on roughened surfaces showed that the velocity profile in the turbulent flow region is strongly dependent upon the roughness height along with the flow Reynolds number. A parameter combining the two (i.e. roughness height and Reynolds number) had been defined and used in roughened surface flow analysis. This parameter is called roughness Reynolds number and is expressed as

$$e^+ = \frac{e}{D}\sqrt{\frac{f}{2}}Re \tag{4}$$

where $e$ is the roughness height and $R$ ($e^+$) is known as momentum transfer function and can be written as

$$R(e^+) = \sqrt{\frac{2}{f}} + 2.5\ln\left(\frac{2e}{D}\right) + 3.75 \tag{5}$$

For roughened circular pipes, momentum transfer function has been used to correlate data on friction. A similar relation for heat transfer in terms of a heat transfer function $G$ ($e^+$) has been developed (Dippery and Sabersky, 1963) which can be expressed as

$$G(e^+) = \left[\frac{f}{2St} - 1\right]\sqrt{\frac{f}{2}} + R(e^+) \tag{6}$$

Experimental data collected on various geometries of rib-roughened surfaces has been utilized for the development of correlation of the form

$$R = R(e^{+}, p/e, \text{ Rib shape}, W/H), \tag{7}$$

$$G = G(e^{+}, p/e, \text{ Rib shape}, W/H) \tag{8}$$

It was however, subsequently realized that the statistical correlations may be better suited for design and is easy to formulate. These correlations can be the function of Reynolds number, Relative pitch ($p/e$), relative roughness height ($e/D$), aspect ratio ($W/H$) and the geometry of the rib.

## 3. Flow pattern

The geometry of the artificial roughness can be of different shapes and orientations. Flow patterns are discussed with respect to different types of artificial roughness elements as below.

### 3.1. Effect of rib

The most important effect produced by the presence of a rib on the flow pattern, is the generation of two flow separation regions, one on each side of the rib. The vortices so generated are responsible for the turbulence and hence the enhancement in heat transfers as well as in the friction losses takes place.

### 3.2. Effect of rib height and pitch

Figs. 1 and 2 (Prasad and Saini, 1988) show the flow pattern downstream of a rib as the rib height and pitch are changed. Due to flow separation downstream of a rib, reattachment of the shear layer does not occur for a pitch ratio of less than about 8. Maximum heat transfer has been found to occur in the vicinity of a reattachment point. It is reasonable to accept that a similar effect can be produced by decreasing the relative roughness pitch ($p/e$) for a fixed relative roughness height ($e/D$). For relative roughness pitch considerably less than about 8, the reattachment will not occur at all resulting in the decrease of heat transfer enhancement. However, an increase in pitch beyond about 10 also results in decreasing the enhancement. It can therefore be concluded that there occurs an optimum combination of pitch and height that will result in maximum enhancement.

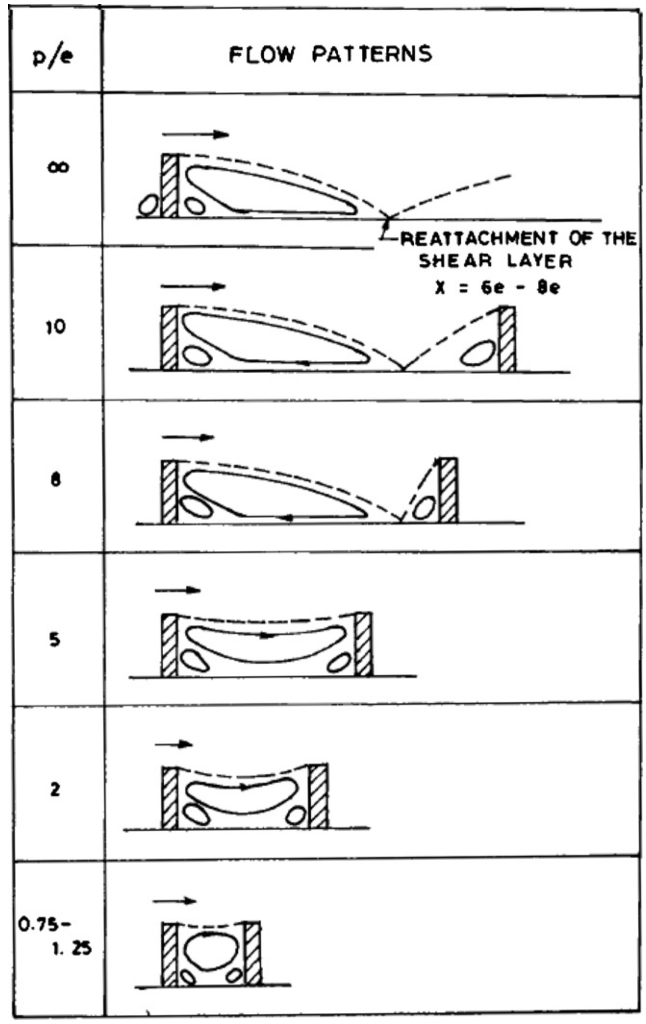


Fig. 1. Flow pattern downstream the roughness as a function of relative roughness pitch.

### 3.3. Effect of inclination of rib

Apart from the effect of rib height and pitch, the parameter that has been found to be most influential is the angle of attack of the flow with respect to the rib position i.e. skewness of rib towards the flow. Span wise counter rotating secondary flows created by angling of the rib, appear to be responsible for the significant span wise variation of heat transfer coefficient. It is pointed out that whereas the two fluid vortices immediately upstream and downstream of a transverse rib are essentially stagnant relative to the mainstream flow which raises the local fluid temperature in the vortices and wall temperature near the rib resulting in low heat transfer. The vortices in the case of angled ribs move along the rib so subsequently join the main stream, the fluid entering near the leading end of rib and coming out near the trailing end (Taslim et al., 1996). These moving vortices therefore bring in cooler channel fluid in contact with leading end raising heat transfer rate while the trailing end heat transfer is relatively lower. This phenomenon therefore results in strong span wise variation of heat transfer.

### 3.4. Effect of V-shaping of rib

The possibility of further enhancing the wall heat transfer by the use of V-shaped ribs is based on the observation of the creation of secondary flow cell due to angling of the rib resulting in a region of higher heat transfer near the

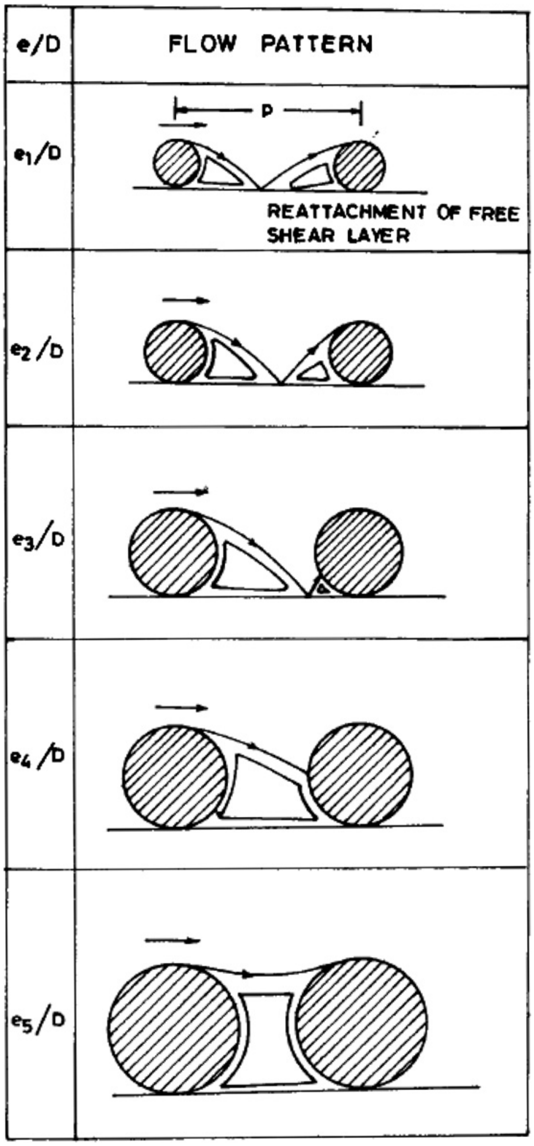


Fig. 2. Flow pattern the roughness as a function of relative roughness height.

leading end. By splitting the long angled rib into a V-shape to form two leading ends and a single trailing end (apex of V), a much larger (about double) region of high heat transfer is produced. It is infact the formation of two secondary flows cells instead of one as in the case of transverse rib that results in higher overall heat transfer in the case of V-shaped ribs.

## 4. Roughness geometries used in heat exchangers

The earlier studies on artificial roughness were carried out in the area of gas turbine airfoil cooling system, gas cooled nuclear reactors and design of compact heat exchangers. Investigators have modeled the shape of internal cooling passage of gas turbine as a rectangular channel with two opposite rough walls and two smooth walls. Several types of surface roughness have been used; they may be broadly classified as regular geometric roughness and irregular roughness. Irregular surface roughness can be produced by sand blasting the surface. Nikuradse (1950) investigated the effect of roughness on the friction factor and velocity distribution in pipes which was roughened by sand blasting. Nunner (1958) and Dippery and Sabersky (1963) developed a friction similarity law and a heat momentum analogy for flow in sand grain roughened tubes.

Regular surface roughness is of many types depending on the shape, arrangement and orientation of roughness elements on the absorber plate. Donne and Meyer (1977), Meyer (1982), Wilkie (1966), Sheriff and Gumley (1966), Gomelauri (1964), Wilkie and Mantle (1979) and Vilemas and Simonis (1985) investigated regular geometric roughness which can be produced in the form of cavities and ribs. Experimental investigations were carried out to study the effect of artificial roughness on heat transfer and friction factor by them.

Sheriff and Gumley (1966) experimentally investigated the optimum roughness Reynolds number ($e^+_{\mathrm{opt}}$) as 35. Burggarf (1970) studied turbulent heat transfer and friction for flow in a square duct with 90° full rib arrays. Ribs, that stretches across the width of the channel at an angle of attack of 90° on two opposite walls and two smooth walls. Han (1984, 1985, 1988), Han et al. (1985, 1988, 1989), Han and Park (1988), Zhang et al. (1984), Zhang and Gu (1994), Chandra et al. (1988), Sparrow and Tao (1984) and Roeller et al. (1991) studied the effects of varying the channel aspect ratio (0.25–4.0), rib angle of attack ($\alpha = 30°$, 45°, 60° and 90°), the rib pitch to height ratio ($p/e = 10$–40), and rib height to channel hydraulic diameter ratio ($e/D = 0.021$–0.063) on the heat transfer in straight square and rectangular channels with full ribs on two opposite walls and two smooth walls. For a square channel, although parallel 60° full ribs enhanced the channel heat transfer the most, they also caused the highest pressure drop. Parallel full ribs having angle of attack, $\alpha$ of 45° and 30° had the best thermal performance. In general parallel angled full ribs enhanced the ribbed wall heat transfer more than the crossed angled full ribs.

Han et al. (1978) reported that ribs inclined at an angle of attack of 45° results in better heat transfer performance when compared to transverse ribs.

Taslim et al. (1991, 1996) studied the augmentation of heat transfer in square channels roughened with rib height to channel hydraulic diameter ($e/D$) in the range of 0.083–0.167 for Reynolds number 5000–30,000. Lau et al. (1991a,b,c) conducted experiments to study the effect of discrete ribs on the turbulent heat transfer and friction for fully developed flow of air in a square channel. Results showed that the average Stanton number for the inclined 45° and 60° discrete ribs was about 20–35% higher than in the 90° full rib case. Han and Zhang (1992) studied the parallel and V-shaped staggered discrete ribs and showed that the 60° staggered discrete V-shaped ribs provided higher heat transfer than that for the parallel discrete ribs and consequently higher than that of other discrete ribs.

Han et al. (1991) investigated the effect of V-shaped ribs and found that V-shaped ribs result in better enhancement in heat transfer in comparison to inclined ribs and transverse ribs.

Hirota et al. (1994) used square ribs and Chang and Mills (1993), Donne and Meyer (1977) and Maubach (1972) used rectangular ribs in their investigations. Ravigururajan and Bergles (1985) used four type of roughness, namely semicircular, circular, rectangular and triangular ribs to develop general statistical correlations for heat transfer and pressure drop for single phase turbulent flow in internally ribbed surface. Liou and Hwang (1992,1993) tested three shapes of rib roughness, namely square, triangular and semicircular ribs to study the effect of rib shapes on turbulent heat transfer and friction in a rectangular channel with two opposite ribbed walls. Hosni et al. (1993) investigated truncated cone roughness, Hosni et al. (1991) used hemisphere roughness elements in a rectangular channel. Kolar (1964) tested screw thread type roughness in pipe flow. Firth and Meyer (1983) investigated the effect of square, helical and trapezoidal rib roughness on heat transfer in annular flow geometry. Williams et al. (1970) used rectangular, chamfered, wedge and helical ribs in a circular annulus flow passage and reported that chamfered and wedge shaped ribs offer relatively lower enhancement in friction losses.

Ichimiya et al. (1991) experimentally investigated the effect of porous type roughness on the heat transfer and friction characteristics in a parallel plate duct. Permeable (porous) rib type roughness are of great interest because they provide a substantially lower drag force in comparison with solid type rib and still provide enhanced heat transfer coefficient in comparison with the smooth wall duct. Hwang and Liou (1994, 1995) experimentally investigated the effects of permeable ribs on heat transfer and friction in a rectangular channel. It was found that permeable ribs gave higher thermal performance than with solid ribs.

Tanasawa et al. (1983) employed the resistance heating method and thermocouple technique to determine the heat transfer coefficients in a channel with turbulence promoters. Three types of turbulence promoter, namely fence type, perforated-plate type and silted plate type were tested. Results showed that the surfaces with perforated plate type turbulence promoters gave an excellent performance under constant pumping power conditions.

Afanasyev et al. (1993) experimentally studied the friction and heat transfer in regular arrays of spherical pits on flat plate and reported that 30–40% heat transfer enhancement without any appreciably effect on the hydrodynamic loss. This investigation however was much localized at mid point (outside of concavity) of a staggered dimpled plate. Belen'kiy et al. (1994) employed staggered array of concave dimples in annular passages on the interior cylindrical surfaces. Heat transfer augmentations as high as 150%, compared to smooth surfaces were reported with appreciable pressure losses. Gortyshov et al. (1998) placed spherical shaped dimples on the opposite surfaces of narrow channel (Chyu et al., 1997). Enhancement of the overall heat transfer rate was about 2.5 times the smooth surface values over a range of Reynolds number. The pressure losses are about half the values produced by conventional rib turbulators. Burgess et al. (2003) experimentally investigated heat transfer and friction factor in rectangular channel having dimples on one wall with an aspect ratio of 8, in the range of Reynolds numbers of 12,000–70,000. Moon et al. (1999) experimentally investigated the heat transfer and friction characteristics of concavities as roughness element on one wall. The heat transfer coefficients were measured using a transient thermo chromic liquid crystal technique. The heat transfer enhancement on the dimpled wall was found approximately 2.1 times that of a smooth channel in the thermally developed region for Reynolds number ranging from 12,000 to 60,000. The thermal performance of dimpled surface was found superior to that of continuous ribs. It was unchanged that with concavities substantial heat transfer can be achieved with a relatively low pressure penalty.

Kesarev and Kozlov (1993) conducted a convective heat transfer test with a single concavity. The study was limited to the concavity inside surface and reported that the total heat flux was about 1.5 times that of a plane circle of the same diameter at a free stream turbulence level of 0.5 level. This study failed to address the heat transfer enhancement outside of the concavity. The potential gas turbine applications of concavity designs were studied by Sehukin et al. (1995).

Lorenz et al. (1995) experimentally investigated the distribution of the heat transfer coefficient in a channel with periodic transverse grooves. Local convective heat transfer coefficients were evaluated from local temperatures taking into account. The global Nusselt number at the grooved wall was found augmented by 1.52–1.75 in comparison to a smooth channel.

For compact design and efficient heat exchangers several investigations have been carried out in roughened circular tubes by Sams (1952), Webb et al. (1972), Webb and Eckert (1972), Webb (1994), Gee and Webb (1980), Brouillette et al. (1957), Koch (1960), Molloy (1967) and Sethumadhavan and Raja Rao (1983). Based on the experimental studies following correlations were developed by Webb et al., 1971 for transverse square ribs for ($e^+ > 25$).

$$R = 0.95(p/e)^{0.53} \tag{9}$$

$$G = 4.5Pr^{0.57}(e^+)^{0.28} \tag{10}$$

A detailed investigations and analysis of compact heat exchangers had been compiled by Kays and London (1964).

## 5. Roughness geometries used in solar air heater ducts

To increase the heat transfer in the case of solar air heaters, the roughness elements have to be considered only on one wall, which is the only heated wall, because there is only one wall, which receives the solar radiation. Therefore, the solar air heaters are modeled as a rectangular channel having one rough wall and three smooth walls. This makes the fluid flow and heat transfer characteristics distinctly different from those found in the case of channel with two opposite roughened walls, roughened annular and circular tubes. Further the range of Reynolds number applicable in solar air heaters are of lower range in comparison of the studies discussed above.

These investigators studied the effect of geometric parameters of roughness elements, on heat transfer and friction factor in gas turbine cooling and heat exchanger applications. However the similar geometries can be used for the lower range of Reynolds number for solar air heater applications. Keeping this in view several investigators investigated various geometries of artificial roughness in solar air heater ducts. Correlations for heat transfer and friction factor were developed based on the experimental study carried out by the various investigators. Different geometries of roughness elements studied by the investigators are discussed in the following sections of the paper.

### 5.1. Small diameter wire

Prasad and Saini (1988) investigated the effect of relative roughness height ($e/D$) and relative roughness pitch ($p/e$) on heat transfer and friction factor. The type and orientation of the geometry is shown in Fig. 3. It has been observed that increase in the relative roughness height results in a decrease of the rate of heat transfer enhancement although the rate of increase of friction factor increases. Increase in the relative roughness pitch results in a decrease in the rate of both heat transfer and friction factor. The maximum enhancement in Nusselt number and friction factor were as 2.38 and 4.25 times than that of smooth duct respectively. The optimal thermohydraulic performance given by Webb and Eckert (1972) [$\eta_{\text{thermo}} = (St_r/St_s)\ /(f_r/f_s)^{1/3}$] (i.e. maximum heat transfer for minimum fluid pressure) could be achieved at $e^+$ of 24.

Gupta et al. (1993) investigated the effect of relative roughness height, angle of attack and Reynolds number on heat transfer and friction factor in rectangular duct having circular wire ribs on the absorber plate. The orientation of the geometry was as shown in Fig. 4. It was found that the heat transfer coefficient in roughened duct could be improved by a factor up to 1.8 and the friction factor had been found to increase by a factor up to 2.7 times of smooth duct. The maximum heat transfer coefficient and friction factor were found at an angle of attack of 60° and 70° respectively in the range of parameters investigated. The thermohydraulic performance of roughened surfaces had been found best corresponding relative roughness height $e/D$ of 0.033 and the Reynolds number corresponding to the best thermohydraulic performance were around 14,000 in the range of parameters investigated.

Verma and Prasad (2000) also investigated the effect of similar geometrical parameters of circular wire ribs on heat transfer and friction factor. It was observed that the value of heat transfer enhancement factor ($Nu_r/Nu_s$) varies from 1.25 to 2.08 within the range of parameters investigated. It was also found that for roughness Reynolds number ($e^+$) of 24, the thermohydraulic performance in such collector was maximum. The value of optimal thermohydraulic performance had been found to be about 71% corresponding to $e^+$ of 24.

### 5.2. Expanded metal mesh

Saini and Saini (1997) investigated the effect of expanded metal mesh geometry as shown in Fig. 5, the effect of relative long way length of mesh ($l/e$) and relative short way length of mesh ($s/e$) on heat transfer and friction factor. The maximum Nusselt number and friction factor were found corresponding to relative long way length of mesh of 46.87 and 71.87 respectively for all the values of relative short way length of mesh investigated. The maximum Nusselt number and friction factor occur for relative short way length of mesh of 25 and 15 respectively. The maximum enhancement in Nusselt number and friction factor values were reported of the order of 4 and 5 times to the smooth plate respectively.

### 5.3. V-Shaped ribs

Muluwork et al. (1998) compared the thermal performance of staggered discrete V-apex up and down with corresponding transverse staggered discrete ribs as shown in Fig. 6. The relative roughness length ratio ($g/p$) had been

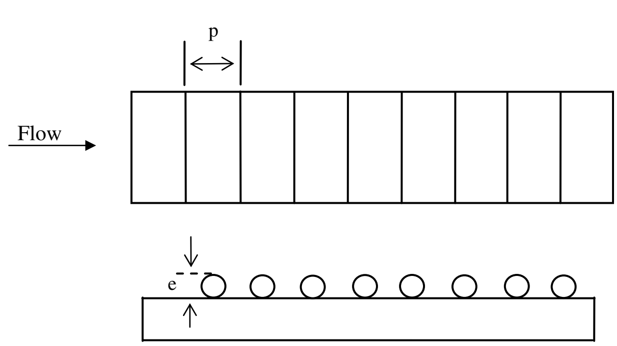


Fig. 3. Type and orientation of roughness element investigated by Prasad and Saini (1988).

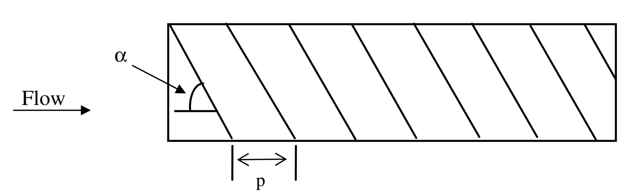


Fig. 4. Orientation of roughness element investigated by Gupta et al. (1993).

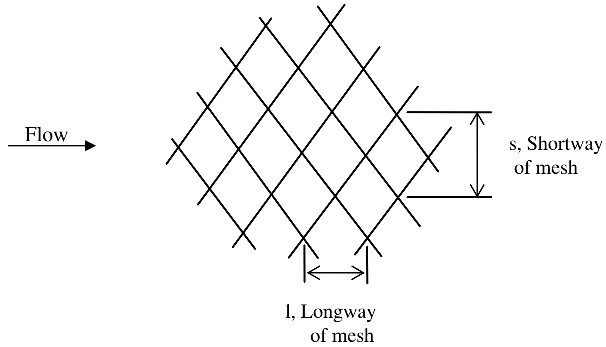


Fig. 5. Orientation of roughness element investigated by Saini and Saini (1997).

considered as dimensionless geometric parameter of roughness element to compare three different configurations. It was observed that the Stanton number increases with the increase of relative roughness length ratio. The Stanton number for V-down discrete ribs was higher than the corresponding V-up and transverse discrete roughened surfaces. The Stanton number ratio enhancement was found 1.32–2.47 in the range of parameters covered in the investigation. It was also observed that the friction factor increases with an increase in the relative roughness length ratio. Further for Stanton number, it was seen that the ribbed surface friction factor for V-down discrete ribs was highest among the three configurations investigated.

Momin et al. (2002) experimentally investigated the effect of geometrical parameters of V-shaped ribs on heat transfer and fluid flow characteristics in rectangular duct of solar air heater. The investigated geometry was as shown in Fig. 7. The investigation covered Reynolds number range of 2500–18,000, relative roughness height of 0.02–0.034 and angle of attack of flow ($\alpha$) of 30–90° for a fixed relative pitch of 10. For this geometry it was observed that the rate of increase of Nusselt number with an increase in Reynolds number is lower than the rate of increase of friction factor. The maximum enhancement of Nusselt number and friction factor as result of providing artificial roughness had been found as 2.30 and 2.83 times to smooth surface respectively for an angle of attack of 60°. It was also found that for relative roughness height of 0.034 and angle of attack of 60°, the V-shaped ribs enhance the value of Nusselt number by 1.14 and 2.30 times over inclined ribs and smooth plate respectively. It was concluded that V-shaped ribs gave better heat transfer performance than the inclined ribs for similar operating conditions.

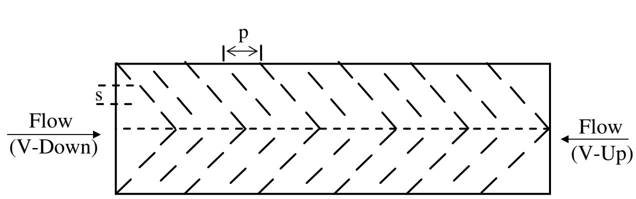


Fig. 6. Orientation of roughness element investigated by Muluwork et al. (1998).

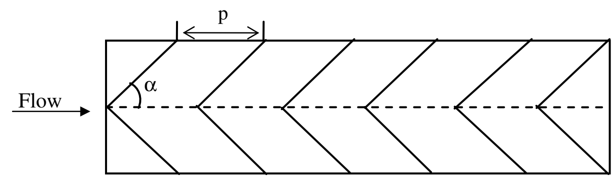


Fig. 7. Orientation of roughness element investigated by Momin et al. (2002).

### 5.4. Chamfered ribs

Karwa et al. (1999) performed experimental study to predict the effect of rib head chamfer angle ($\phi$) and duct aspect ratio on heat transfer and friction factor in a rectangular duct roughened with integral chamfered ribs as shown in Fig. 8. As compared to the smooth duct, the presence of chamfered ribs on the wall of duct yields up to about twofold and threefold increase in the Stanton number and the friction factor respectively in the range of parameters investigated. The highest heat transfer as well as highest friction factor exists for a chamfer angle ($\phi$) of 15°. The minima of the heat transfer function occur at roughness Reynolds number of about 20. As the aspect ratio ($H/D$) increases from 4.65 to 9.66, the heat transfer function also increases and then attains nearly a constant value. The roughness function decreases with the increase

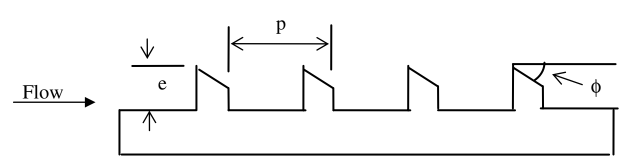


Fig. 8. Type of roughness element investigated by Karwa et al. (1999).

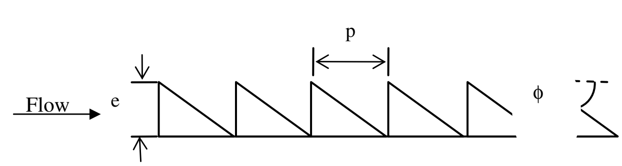


Fig. 9. Type of roughness element investigated by Bhagoria et al. (2002).

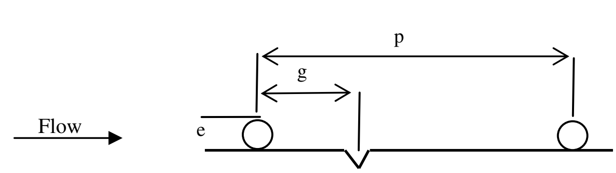


Fig. 10. Type of roughness element investigated by Jaurker et al. (2006).

Table 1
Correlations developed for heat transfer coefficient and friction factor for different roughness geometries used in solar air heater duct

| Authors | Type of roughness | Range of parameters | Correlations: Heat transfer coefficient | Correlations: Friction factor |
|---|---|---|---|---|
| Prasad and Saini (1988) | Small diameter protrusion wire | $e/D$: 0.020–0.033<br>$p/e$: 10–20<br>$Re$: 5000–50,000 | $\bar{S}t = \dfrac{\bar{f}/2}{1+\sqrt{\bar{f}/2}\left\{4.5(e^{+})^{0.28}Pr^{0.57} - 0.95(p/e)^{0.53}\right\}}$ | $\bar{f} = \dfrac{(W+2B)f_s + Wf_r}{2(W+B)}$<br>where<br>$f_r = \dfrac{2}{[0.95(p/e)^{0.53} + 2.5\ln(D/2e) - 3.75]^2}$ |
| Gupta et al. (1993) | Angled circular rib | $e/D$: 0.020–0.053<br>$p/e$: 7.5 & 10<br>$\alpha$: 30–90°<br>$Re$: 5000–30,000 | $Nu_r = 0.0024(e/D)^{0.001}(W/H)^{-0.06}Re^{1.084} \times \exp[-0.04(1-\alpha/60)^2]$ for $e^{+} < 35$<br>$Nu_r = 0.0071(e/D)^{-024}(W/H)^{-0.028}Re^{0.88} \times \exp[-0.475(1-\alpha/60)^2]$ for $e^{+} > 35$ | $f_r = 0.1911(e/D)^{0.196}(W/H)^{-0.093}Re^{-0.165} \times \exp[-0.993(1-\alpha/70)^2]$ |
| Verma and Prasad (2000) | Circular ribs | $e/D$: 0.01–0.03<br>$Re$: 5000–20,000<br>$p/e$: 10–40<br>$e^{+}$: 8–42 | $Nu_r = 0.08596(p/e)^{-0.054}(e/D)^{0.072}Re^{0.723}$ for $e^{+} \leqslant 24$<br>$Nu_r = 0.02954(p/e)^{-0.016}(e/D)^{0.021}Re^{0.802}$ for $e^{+} > 24$ | $f_r = 0.245(p/e)^{-0.206}(e/D)^{0.243}Re^{-1.25}$ |
| Saini and Saini (1997) | Expanded metal mesh | $e/D$: 0.012–0.039<br>$S/e$ : 15.62 – 46.87<br>$L/e$: 25.00–71.87<br>$Re$: 1900–13,000 | $Nu_r = 4.0 \times 10^{-4}Re^{1.22}(e/D)^{0.625}(s/10e)^{2.22}\exp[-1.25\{\ln(s/10e)\}^2]$ $(l/10e)^{2.66} \times \exp[-0.824\{\ln(l/10e)\}^2]$ | $f_r = 0.815Re^{-0.361}(l/e)^{0.266}(s/10e)^{-0.19}(10e/D)^{0.591}$ |
| Muluwork et al. (1998) | V-Shaped staggered discrete rib | $B/S$: 3–9<br>$\alpha$: 60°<br>$e/D$: 0.02<br>$Re$: 2000–15,500 | $Nu_r = 0.00534Re^{1.2991}(p/S)^{1.3496}$ | $f_r = 0.7117Re^{-2.991}(p/S)^{0.0636}$ |
| Momin et al. (2002) | V-Shaped rib | $e/D$: 0.02–0.034<br>$p/e$: 10<br>$\alpha$: 30–90<br>$Re$: 2500–18,000 | $Nu_r = 0.067Re^{0.888}(e/D)^{0.424}(\alpha/60)^{-0.077} \times \exp[-0.782\{\ln(\alpha/60)\}^2]$ | $f_r = 6.266Re^{-0.425}(e/D)^{0.565}(\alpha/60)^{-0.093} \times \exp[-0.719\{\ln(\alpha/60)\}^2]$ |
| Karwa et al. (1999) | Chamfered rib | $W/H$: 4.8, 6.1, 7.8, 9.66, 12.0<br>$e/D$: 0.014–0.0328<br>$p/e$ : 4.5, 5.8, 7, 8.5<br>$\phi$: −15, 0, 10, 15, 18<br>$Re$: 3000–20,000 | $G = 103.77e^{-0.006\phi}(W/H)^{0.5}(p/e)^{2.56} \times \exp[0.7343\{\ln(p/e)\}^2](e^{+})^{-0.31}$ for $7 \leqslant e^{+} < 20$<br>$G = 32.56e^{-0.006\phi}(W/H)^{0.5}(p/e)^{2.56} \times \exp[0.7343\{\ln(p/e)\}^2](e^{+})^{0.08}$ for $20 < e^{+} \leqslant 60$ | $R = 1.66e^{-0.0078\phi}(W/H)^{-0.4}(p/e)^{2.695} \times \exp[-0.762\{\ln(p/e)\}^2](e^{+})^{-0.075}$ for $7 \leqslant e^{+} < 20$<br>$R = 1.325e^{-0.0078\phi}(W/H)^{-0.4}(p/e)^{2.695} \times \exp[-0.762\{\ln(p/e)\}^2]$ for $20 < e^{+} \leqslant 60$ |

| | | | | |
|---|---|---|---|---|
| Bhagoria et al. (2002) | Wedge shaped rib | $e/D$: 0.015–0.033<br>$p/e$: $60.17\phi^{-1.0264} <$<br>$p/e < 12.12$<br>$\phi$: 8, 10, 12, 15<br>$Re$: 3000–18,000 | $Nu_r = 1.89 \times 10^{-4} Re^{1.21} (e/D)^{0.426} (p/e)^{2.94} \times \exp[-0.71\{\ln(p/e)\}^2] (\phi/10)^{-0.018} \times \exp[-1.5\{\ln(\phi/10)\}^2]$ | $f_r = 12.44 Re^{-0.18} (e/D)^{0.99} (p/e)^{-0.52} (\phi/10)^{0.49}$ |
| Jaurker et al. (2006) | Rib-grooved | $e/D$: 0.0181–0.0363<br>$p/e$: 4.5–10<br>$Re$: 3000–21,000<br>$g/p$: 0.3–0.7 | $Nu_r = 0.002062 Re^{0.936} (e/D)^{0.349} (p/e)^{3.318} \times \exp[-0.868\{\ln(p/e)\}^2] (g/p)^{1.108} \times \exp[2.486\{\ln(g/p)^2\} + 1.406\{\ln(g/p)^3\}]$ | $f_r = 0.001227 Re^{-0.199} (e/D)^{0.585} (p/e)^{7.19} \times \exp[-1.854\{\ln(p/e)\}^2] (g/p)^{0.645} \times \exp[1.513\{\ln(g/p)^2\} + 0.8662\{\ln(g/p)^3\}]$ |

in the aspect ratio ($H/D$) from 4.65 to 7.75 and then attains nearly a constant value.

### 5.5. Wedge shaped ribs

Bhagoria et al. (2002) performed experiments to determine the effect of relative roughness pitch, relative roughness height and wedge angle on the heat transfer and friction factor in a solar air heater roughened duct having wedge shaped rib roughness as shown in Fig. 9. The presence of ribs yields Nusselt number up to 2.4 times while the friction factor rises up to 5.3 times as compared to smooth duct in the range of parameters investigated. A maximum enhancement in heat transfer was obtained at a wedge angle of about 10°. The heat transfer was found maximum for a relative roughness pitch of about 7.57. The friction factor was decreased as the relative roughness pitch increased.

Sahu and Bhagoria (2005) experimentally investigated similar geometry having broken transverse ribs in solar air heaters. The investigation covered Reynolds number range of 3000–12,000, roughness pitch of 10–30 mm, height of the rib 1.5 mm and the aspect ratio of 8. it was found out that the maximum Nusselt number attained for roughness pitch ($p/e$) of 20 and decreased with an increase in roughness pitch. Roughened absorber plates increased the heat transfer coefficient by 1.25–1.4 times as compared to smooth rectangular duct under similar operating conditions at higher Reynolds number. Based on experimentation it was concluded that the maximum thermal efficiency of roughened solar air heater was to be of the order of (51–83.5%) depending upon the flow conditions.

### 5.6. Combination of different roughness elements

Jaurker et al. (2006) experimentally investigated the heat transfer and friction characteristics of rib-grooved artificial roughness on one broad wall as shown in Fig. 10. The effect of relative roughness pitch, relative roughness height and relative groove position on the heat transfer coefficient and friction factor was studied. The maximum heat transfer was obtained for a relative roughness pitch of about 6, and it was decreased either side of relative roughness pitch. The optimum condition for heat transfer was found at a groove position to pitch ratio of 0.4.

Based on the experimental studies carried out by various investigators, correlation for Nusselt number and friction factor were developed. These correlations along with the range of parameters investigated are given in Table 1.

## 6. Conclusions

It can be concluded from the present review that lot of work has been carried out to investigate the effect of artificial roughness of different shapes and sizes on heat transfer and friction factor. Substantial enhancement in the heat transfer can be achieved with little penalty of friction.

Various investigators have developed correlations for heat transfer and friction factor for solar air heater ducts having artificial roughness of different geometries. These correlations can be used to predict the thermal as well as thermo-hydraulic performance of solar air heaters having roughened ducts.

## References


Afanasyev, V.N., Chudnovsky, Y.P., Leontiev, A.I., Roganov, P.S., 1993. Turbulent flow friction and heat transfer characteristics for spherical cavities on a flat plate. Experimental Thermal Fluid Science 7, 1–8.

Belen'kiy, M.Y., Gotovskiy, M.A., Lekakh, B.M., Fokin, B.S., Dolgushin, K.S., 1994. Heat transfer augmentation using surfaces formed by a system of spherical cavities. Heat Transfer Research 25 (2), 196–203.

Bhagoria, J.L., Saini, J.S., Solanki, S.C., 2002. Heat transfer coefficient and friction factor correlations for rectangular solar air heater duct having transverse wedge shaped rib roughness on the absorber plate. Renewable Energy 25, 341–369.

Brouillette, E.D., Mefflin, T.L., Myers, J.E., 1957. Heat transfer and pressure drop characteristics at internal finned tubes. ASME paper; 57-A-47.

Burgess, N.K., Oliveira, M.M., Ligrani, P.M., 2003. Nusselt number behavior on deep dimpled surfaces within a channel. Journal of Heat Transfer 125, 11–18.

Burggarf, F., 1970. Experimental heat transfer and pressure drop with two-dimensional turbulence promoter applied to two opposite walls of a square tube. In: Bergles, E., Webb, R.L. (Eds.), Augmentation of Heat and Mass Transfer. ASME, New York, pp. 70–79.

Chandra, P.R., Han, J.C., Lau, S.C., 1988. Effect of rib angle on local heat/mass transfer distributions in two-pass rib-roughened channel. ASME Journal of Turbomachinery 110, 233–241.

Chang, B.H., Mills, A.F., 1993. Turbulent flow in a channel with transverse rib heat transfer augmentation. International Journal of Heat and Mass Transfer 36, 1459–1469.

Chyu, M.K., Yu, Y., Ding, H., 1997. Concavity enhanced heat transfer in an internal cooling passage. ASME paper 97-GT-437.

Dippery, D.F., Sabersky, R.H., 1963. Heat and momentum transfer in smooth and rough tubes at various Prandtl number. International Journal Heat and Mass Transfer 6, 329–353.

Donne, D., Meyer, L., 1977. Turbulent convective heat transfer from rough surfaces with two dimensional rectangular ribs. International Journal of Heat and Mass Transfer 20, 582–620.

Firth, R.J., Meyer, L., 1983. A comparison of the heat transfer and friction factor performance of four different types of artificially roughened surface. International Journal of Heat and Mass Transfer 26 (2), 175–183.

Gee, D.L., Webb, R.L., 1980. Forced convection heat transfer in helically rib-roughened tubes. International Journal of Heat and Mass Transfer 23, 1127–1136.

Gomelauri, V., 1964. Influence of two-dimensional artificial roughness on convective heat transfer. International Journal of Heat and Mass Transfer 7, 653–663.

Gortyshov, Y.F., Popov, I.A., Amirkhanov, R.D., Gulitsky, K.E., 1998. Studies of hydrodynamics and heat exchange in channels with various types of intensifiers. In: Proceedings of 11th International Heat Transfer Congress, Vol. 6. p. 83–88.

Gupta, D., Solanki, S.C., Saini, J.S., 1993. Heat and fluid flow in rectangular solar air heater ducts having transverse rib roughness on absorber plates. Solar Energy 51, 31–37.

Han, J.C., 1984. Heat transfer and friction in channels with two opposite rib-roughened walls. ASME Journal of Heat Transfer 106, 774–781.

Han, J.C., 1985. Heat transfer enhancement in channels with turbulence promoters. Journal of Engineering for Gas Turbines and Power 107, 628–635.

Han, J.C., 1988. Heat transfer and friction characteristics in rectangular channels with rib turbulators. ASME Journal of Heat Transfer 110, 321–328.

Han, J.C., Park, J.S., 1988. Developing heat transfer in rectangular channels with rib turbulators. International Journal of Heat and Mass Transfer 31, 183–195.

Han, J.C., Zhang, Y.M., 1992. High performance heat transfer ducts with parallel, broken and V-shaped broken ribs. International Journal of Heat and Mass Transfer 35 (2), 513–523.

Han, J.C., Glicksman, L.R., Rohsenow, W.M., 1978. An investigation of heat transfer and friction for rib-roughened surfaces. International Journal of Heat and Mass Transfer 21, 1143–1156.

Han, J.C., Park, J.S., Lei, C.K., 1985. Heat transfer enhancement in channels with turbulence promoters. ASME Journal of Engineering for Gas Turbines and Power 107, 629–635.

Han, J.C., Chandra, P.R., Lau, S.C., 1988. Local heat/mass transfer distributions around sharp 180° turns in two-pass smooth and rib-roughened channel. ASME Journal of Heat Transfer 110, 91–98.

Han, J.C., Ou, S., Park, J.S., Lei, C.K., 1989. Augmented heat transfer in rectangular channels with narrow aspect ratios with rib turbulators. International Journal of Heat and Mass Transfer 32, 1619–1630.

Han, J.C., Zhang, Y.M., Lee, C.P., 1991. Augmented heat transfer in square channels with parallel, crossed, and V-shaped angled ribs. ASME Journal of Heat Transfer 113, 590–596.

Hirota, M., Fuzita, H., Yokosawa, H., 1994. Experimental study on convective heat transfer for turbulent flow in a square duct with a ribbed wall (characteristics of mean temperature field). ASME Journal of Heat Transfer 116, 332–340.

Hosni, M.H., Coleman, H.W., Taylor, R.P., 1991. Measurements and calculations of rough-wall heat transfer in the turbulent boundary layer. International Journal of Heat and Mass Transfer 34, 1067–1082.

Hosni, M.H., Coleman, H.W., Garner, J.W., Taylor, R.P., 1993. Roughness element shape effects on heat transfer and skin friction in rough-wall turbulent boundary layers. International Journal of Heat and Mass Transfer 36, 147–153.

Hwang, J.J., Liou, T.M., 1994. Augmented heat transfer in a rectangular channel with permeable ribs mounted on the wall. ASME Journal of Heat Transfer 116, 912–920.

Hwang, J.J., Liou, T.M., 1995. Effect of permeable ribs on heat transfer and friction in a rectangular channel. ASME Journal of Turbomachinery 117, 265–271.

Ichimiya, K., Katayama, M., Miyazawa, T., Kondoh, H., 1991. Experimental study on effects of a single porous type roughness element in a parallel plate duct. Experimental Heat Transfer 4, 319–330.

Jaurker, A.R., Saini, J.S., Gandhi, B.K., 2006. Heat transfer and friction characteristics of rectangular solar air heater duct using rib-grooved artificial roughness. Solar Energy 80 (8), 895–907.

Karwa, R., Solanki, S.C., Saini, J.S., 1999. Heat transfer coefficient and friction factor correlations for the transitional flow regime in rib-roughened rectangular ducts. International Journal of Heat and Mass Transfer 42, 1597–1615.

Kays, W.M., London, A.L., 1964. Compact Heat Exchangers. McGraw Hill, New York.

Kesarev, V.S., Kozlov, A.P., 1993. Convective heat transfer in turbulized flow past a hemispherical cavity. Heat Transfer-Soviet Research 25 (2), 156–160.

Koch, R., 1960. Pressure loss and heat transfer for turbulent flow. English Translation. AEC-Tr-3875.

Kolar, V., 1964. Heat transfer in turbulent flow of fluids through smooth and rough tubes. International Journal of Heat and Mass Transfer 8, 639–653.

Lau, S.C., Kukraja, R.T., McMillin, R.D., 1991a. Effect of V-shaped rib arrays on turbulent heat transfer and friction of fully developed flow in a square channel. International Journal of Heat and Mass Transfer 34, 1605–1616.

Lau, S.C., McMillin, R.D., Han, J.C., 1991b. Heat transfer characteristics of turbulent flow in a square channel with angle discrete ribs. ASME Journal of Turbomachinery 113, 367–374.

Lau, S.C., McMillin, R.D., Han, J.C., 1991c. Turbulent heat transfer and friction in a square channel with discrete rib turbulators. ASME Journal of Turbomachinery 113, 360–366.

Liou, T.M., Hwang, J.J., 1992a. Turbulent heat transfer and friction in periodic fully developed channel flows. ASME Journal of Turbomachinery 114, 56–64.

Liou, T.M., Hwang, J.J., 1992b. Developing heat transfer and friction in a rectangular ribbed duct with flow separation at inlet. ASME Journal of Heat Transfer 114, 565–573.

Liou, T.M., Hwang, J.M., 1993. Effect of ridge shapes on turbulent heat transfer and friction in a rectangular channel. International Journal of Heat and Mass Transfer 36, 931–940.

Lorenz, S., Mukomilow, D., Leiner, W., 1995. Distribution of the heat transfer coefficient in a channel with periodic transverse grooves. Experimental Thermal and Fluid Sciences 11, 234–242.

Maubach, K., 1972. Rough annulus pressure drop interpretation of experiments and recalculation for square ribs. International Journal of Heat and Mass Transfer 15, 2489–2498.

Meyer, L., 1982. Thermohydraulic characteristics of single rods with three dimensional roughness. International Journal of Heat and Mass Transfer 25, 1043–1058.

Molloy, J., 1967. Rough tube friction factors and heat transfer coefficients in laminar and transition flow. UKAEA AERE-R5415.

Momin, A.-M.E., Saini, J.S., Solanki, S.C., 2002. Heat transfer and friction in solar air heater duct with V-shaped rib roughness on absorber plate. International Journal of Heat and Mass Transfer 45, 3383–3396.

Moon, H.K., O'Connell, T., Glezer, B., 1999. Channel height effect on heat transfer and friction in a dimpled passage. Journal of Engineering for Gas Turbines and Power 122, 307–313.

Muluwork, K.B., Saini, J.S., Solanki, S.C., 1998. Studies on discrete RIB roughened solar air heaters. In: Proceedings of National Solar Energy Convention, Roorkee; pp. 75–84.

Nikuradse, J., 1950. Laws of flow in rough pipes. NACA, Technical Memorandum 1292. November 1950.

Nunner, W., 1958. Heat transfer and pressure drop in rough tubes. VDI Forch 445-B 5-39 (1956); AERE Lib Trans. 786.

Prasad, B.N., Saini, J.S., 1988. Effect of artificial roughness on heat transfer and friction factor in a solar air heater. Solar Energy 41 (6), 555–560.

Ravigururajan, T.S., Bergles, A.E., 1985. General correlation for pressure drop and heat transfer for single phase turbulent flow in internally ribbed tubes. Augmentation of Heat Transfer in Energy Systems. HTD 52. ASME, New York, pp. 9–20.

Roeller, P.T., Stevens, J., Webb, B.W., 1991. Heat transfer and turbulent flow characteristics of isolated three dimensional protrusions in channels. ASME Journal of Heat Transfer 113, 597–603.

Sahu, M.M., Bhagoria, J.L., 2005. Augmentation of heat transfer coefficient by using 90° broken transverse ribs on absorber plate of solar air heater. Renewable Energy 30, 2057–2063.

Saini, R.P., Saini, J.S., 1997. Heat transfer and friction factor correlations for artificially roughened ducts with expanded metal mesh as roughened element. International Journal of Heat and Mass Transfer 40 (4), 973–986.

Sams, E.W., 1952. Experimental investigation of average heat transfer and friction coefficients for air flowing circular pipes having square-thread type roughness. NACA RM; E52–D17.

Sehukin, A.V., Kozlov, A.P., Agachev, R.S., 1995. Study and application of hemispherical cavities for surface heat transfer augmentation. ASME paper 95-GT-59.

Sethumadhavan, R., Raja Rao, M., 1983. Turbulent flow heat transfer and fluid friction in helical-wire-coil-inserted tubes. International Journal of Heat and Mass Transfer 26, 1833–1844.

Sheriff, N., Gumley, P., 1966. Heat transfer and friction properties of surfaces with discrete roughness. International Journal of Heat and Mass Transfer 9, 1297–1320.

Sparrow, E.M., Tao, W.Q., 1984. Symmetric vs asymmetric periodic disturbances at the walls of a heated flow passage. International Journal of Heat and Mass Transfer 27, 2133–2144.

Tanasawa, L., Nishio, S., Tanano, K., Tado, M., 1983. Enhancement of forced convection heat transfer in rectangular channel using turbulence promoters. In: Proceedings of ASME-JSME Thermal Engineering Joint Conference; pp. 395–402.

Taslim, M.E., Bondi, L.A., Kercher, D.M., 1991. An Experimental investigation of heat transfer in an orthogonally rotating channel roughened with 45°. Criss-cross ribs on two opposite walls. ASME Journal of Turbomachinery 113, 346–353.

Taslim, M.E., Li, T., Kercher, D.M., 1996. Experimental heat transfer and friction in channels roughened with angled, V-shaped and discrete ribs on two opposite walls. ASME Journal of Turbomachinery 118, 20–28.

Verma, S.K., Prasad, B.N., 2000. Investigation for the optimal thermohydraulic performance of artificially roughened solar air heaters. Renewable Energy 20, 19–36.

Vilemas, J.V., Simonis, V.M., 1985. Heat transfer and friction of rough ducts carrying gas flow with variable physical properties. International Journal of Heat and Mass Transfer 28, 59–68.

Webb, R.L., 1994. Principles of Enhanced Heat Transfer. John Wiley and Sons, New York.

Webb, R.L., Eckert, E.R.G., 1972. Application of rough surfaces to heat exchanger design. International Journal of Heat and Mass Transfer 15, 1647–1658.

Webb, R.L., Eckert, E.R.G., Goldstein, R.J., 1971. Heat transfer and friction in tubes with repeated-rib roughness. International Journal of Heat and Mass Transfer 14, 601–617.

Webb, R.L., Eckert, E.R.G., Goldstein, R.J., 1972. Generalized heat transfer and friction correlations for tubes with repeated rib roughness. International Journal of Heat and Mass Transfer 15, 180–183.

Wilkie, D., 1966. Forced convection heat transfer from surfaces roughened by transverse ribs. In: Proceedings of the 2nd International Heat Transfer Conference, Vol. 1, AIChE, New York.

Wilkie, D., Mantle, P.L., 1979. Multi-start helically ribbed fuel pins for CAGR. Nuclear Energy 18, 277–282.

Williams, F., Pirie, M.A.M., Warburton, C., 1970. Heat transfer from surface roughened by ribs. In: Bergles, A., Webb, R.L. (Eds.), Augmentation of Heat and Mass Transfer. ASME, New York, pp. 36–43.

Zhang, Y.M., Gu, W.Z., 1994. Heat transfer and friction in rectangular channels with ribbed or ribbed-grooved walls. ASME Journal of Heat Transfer 116, 58–65.

Zhang, Y.M., Gu, W.Z., Xu, H.Q., 1984. Enhancement of heat transfer and flow characteristics in rib roughened rectangular channels. Journal of Engineering Thermophysics 5 (3), 275–280.